COMMUNICATION

Check for updates

The CF₃TMS adduct of anthraquinone as a monomer for making polymers with potential as separation membranes†

Kim Jiayi Wu, [ID] [a] John M. Tobin,[a] Anli Ji,[a] Yang Shi,[a] Chunchun Ye,[a] Gary S. Nichol, [ID] [a] Alessio Fuoco, [ID] [b] Mariagiulia Longo,[b] Johannes C. Jansen [ID] [b] and Neil B. McKeown [ID] *[a]

The readily prepared CF₃TMS adduct of anthraquinone is shown to be an efficient monomer for superacid-catalysed step-growth polymerisations, as exemplified by its reaction with diphenyl ether. The resulting polymer (BTFMA-DPE) is produced rapidly, with high molecular mass, and shows promise as a gas separation membrane material.

Superacid-catalysed step-growth polymerisations have been investigated for over two decades.[1–4] The mechanism of these polymerisations involves the formation of highly reactive carbocations (*i.e.*, superelectrophiles) from a carbonyl-containing monomer, which then react with a bifunctional aromatic monomer that is activated towards aromatic electrophilic substitution. Suitable carbonyl-containing monomers include 1,1,1-trifluoroacetophenone,[5] isatin and its derivatives,[1,6] 4-piperidone,[7] 1,1,1-trifluoroacetone,[6] 4-acetylpyridine,[8,9] and acenaphthenequinone,[10] and suitable aromatic monomers include biphenyl,[2] terphenyl,[10] 4,4′-diphenoxybenzophenone[1] or diphenyl ether[10] (Fig. 1). Typically, the superacid used is trifluoromethylsulfonic acid (TFSA). The attractive features of superacid mediated polymerisations are their use of readily available monomers and rapid completion even at room temperature, allowing for ease of scale-up to multigram quantities or greater. Recently, such polymerisations have been used intensively to prepare membrane materials for application in a wide variety of technologies relevant to energy and environmental sustainability including gas separations,[11–16] water purification,[17,18] acid recovery[19,20] and ion separations.[21,22] For example, post-synthetic modification, such as amine quaternisation for those polymers derived from 4-piperidone[23–25] or the introduction of sulfonate groups,[26,27] induce ion-conduct-

ing properties that make them useful as membranes for devices such as proton exchange fuel cells,[9,27–30] alkaline fuel cells,[26,31–37] redox-flow batteries,[38,39] zinc batteries,[40] ammonia electrosynthesisers,[41] and water electrolysers.[42–44]

In this communication, we describe preliminary results on the use of the readily prepared CF₃TMS adduct of anthraquinone (**BTFMA**, Fig. 2) as an electrophilic monomer for enga-
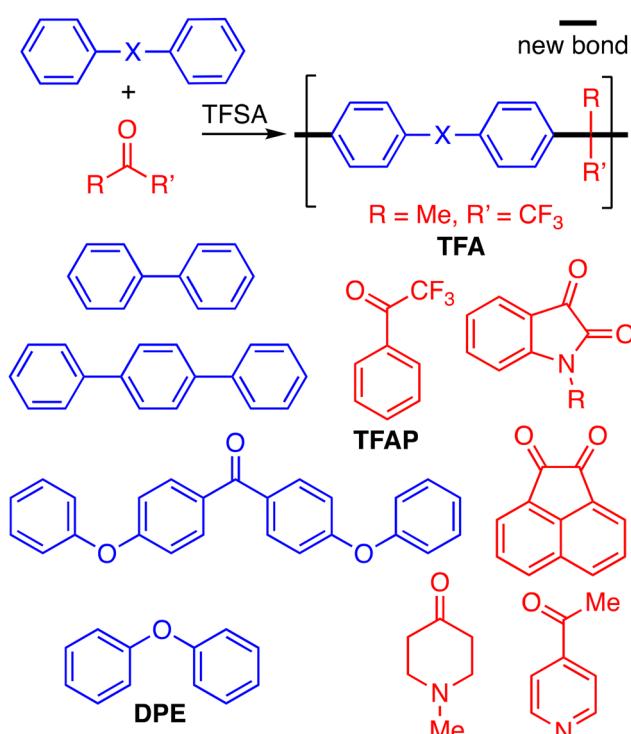
Fig. 1 General scheme of typical superacid polymerisations with examples of suitable electrophilic monomers depicted in blue [biphenyl, terphenyl, diphenyl ether (DPE) and 4,4′-diphenoxybenzophenone] and nucleophilic monomers depicted in red [1,1,1-trifluoroacetone (TFA), 1,1,1-trifluoroacetophenone (TFAP), isatin derivatives, 4-piperidone, acenaphthenequinone and 4-acetylpyridine].

[a] EaStChem, School of Chemistry, University of Edinburgh, David Brewster Road, Edinburgh, EH9 3FJ, UK. E-mail: neil.mckeown@ed.ac.uk
[b] Institute on Membrane Technology, National Research Council of Italy (CNR-ITM), via P. Bucci 17/C, Rende (CS), 87036, Italy
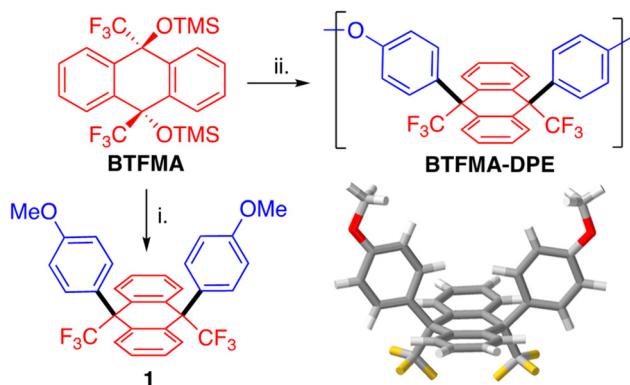
Fig. 2 Synthesis of model compound **1**, shown with its single crystal XRD structure (CCDC 2382285†) confirming its "*cis*" configuration of substituents relative to the anthracene plane, and polymer **BTFMA-DPE**. Reagents and conditions: i. anisole, TFSA, DCM, 20 °C; ii. DPE, TFSA, DCM, 20 °C (90% yield).

ging in superacid mediated polymerisations as exemplified by using diphenyl ether (**DPE**) as co-monomer. The potential of **BTFMA** for making high free volume polymers for membranes is illustrated by an analysis of the gas permeability of the resulting polymer (**BTFMA-DPE**).

Previously, it was reported that two equivalents of trifluoromethyltrimethylsilane (CF$_3$TMS, *i.e.*, the Ruppert–Prakash reagent)[45] add cleanly to anthraquinone to form 9,10-bis(trimethysiloxyl)-9,10-bis(trifluoromethyl)-9,10-dihydroanthracene (**BTFMA**) in high yield.[46,47] On repeating this reaction, it was found that **BTFMA** could be purified easily, without using column chromatography, by simple recrystallisation from isopropanol to give multigram quantities of the adduct as an air-stable, white crystalline solid. Although **BTFMA** has been used previously as an intermediate to produce 9,10-bis(trifluoromethyl)anthracene[48] and monomers for polyimide synthesis,[49,50] we anticipated that it would engage directly in superacid-catalysed aromatic electrophilic substitution reactions with suitably reactive aromatic monomers. Encouragingly, the reaction between **BTFMA** and an excess of anisole, using TFSA as the superacid, gave a high crude yield of 9,10-bis(4′-methoxyphenyl)-9,10-bis(trifluoromethyl)-9,10-dihydroanthracene **1**. It should be noted that previous uses of **BTFMA** as a synthetic intermediate involved the initial removal of the TMS group, *via* aqueous acid hydrolysis, but this proved unnecessary. Indeed, the use of the hydrolysed intermediate (*i.e.*, 9,10-dihydroxy-9,10-bis(trifluoromethyl)-9,10-dihydroanthracene), resulted in a lower yield of model compound **1**. Previous studies have also shown the benefit of using –OTMS as the leaving group for the generation of highly reactive carbocations using a superacid, which avoids the generation of water as by-product that may result in a reduction of the efficiency of TFSA.[51,52] Single-crystal XRD analysis of **1** confirmed the structure of the model compound and revealed that it is composed of the "*cis*" isomer, in which the two CF$_3$ substituents are placed facing the same direction relative to the anthracene plane (Fig. 2). Similar regioselectivity has been

observed previously for closely related superacid mediated reactions.[53] The ^{1}H NMR of **1** obtained at ∼20 °C is deceptively simple as it shows only three peaks in the aromatic region with each of these peaks integrating to 4H relative to the 6H of the methoxy peak. Variable-temperature ^{1}H NMR (ESI Fig. 1†) reveals that the apparently "missing" hydrogen peaks of the anisole substituents are discernible at higher and lower temperatures but are severely broadened at ambient temperature. This effect is due to the restricted rotation about the newly formed C–C bond (see discussion below).

The high yield obtained for the synthesis of model compound **1**, suggested that similar TFSA mediated reactions between **BTFMA** and diphenyl ether (**DPE**) would provide a polymer, denoted as **BTFMA-DPE** (Fig. 2). After an aqueous work-up, fibrous colourless products are obtained that are fully soluble in chloroform. Analysis by gel permeation chromatography (GPC) of the product from polymerisation reactions carried out over a range of conditions (ESI Fig. 2 and Table 1†) showed that high molecular mass **BTFMA-DPE** is formed rapidly (∼0.5 h) at room temperature. For each reaction, two distinct peaks are observed by GPC: one at high molecular mass and one at low molecular mass, the latter with an apparent mass average molecular mass (M_n) of ∼2000 g mol^{-1}, which is assumed to be due to cyclic and/or linear oligomers (ESI Fig. 2†).[54] The relative height of the two peaks is dependent on the reaction conditions with deviations from the 1 : 1 stoichiometry of monomers and lower concentration of reactants enhancing the relative height of the peak attributed to oligomers. For optimised reaction conditions, consisting of 1 : 1 molar stoichiometry, high concentration and a short reaction time (0.5 h), the peak attributed to higher molecular mass polymer is >5 times greater in height relative to than that attributed to the oligomers. The value of M_n calculated from the higher molecular mass peak, following calibration using polystyrene standards, is 150 000 g mol^{-1} with a polydispersity index that is consistent with a standard step-growth mechanism (*i.e.*, M_w/M_n = ∼2). Reprecipitation from chloroform solution using methanol reduces the amount of oligomeric material present in the polymeric product. By using these optimised reaction conditions, samples of **BTFMA-DPE** have been achieved rapidly and reproducibly on a multigram scale (to date up to 30 g). In contrast with previously reported superacid catalysed polymerisations, where a stoichiometric imbalance in favour of the electrophilic monomer results in higher molecular mass, a 1 : 1 molar equivalence of **BTFMA** and **DPE** appears optimal. Previously reported non-stoichiometric enhancement of the polymerisation was attributed to the higher reactivity of the intermediate formed after the first addition of the nucleophilic monomer.[55] Therefore, for **BTFMA** it appears that the reactivity of the carbocation formed following the first addition of **DPE** is similar to that of the initially formed carbocation.

Analysis by ^{1}H- and ^{13}C-NMR, with assignment of protons assisted by ^{1}H-COSY, ^{1}H/^{13}C-HSQC, and ^{1}H/^{13}C-HMBC spectra (Fig. 3 and ESI Fig. 3–5†), confirmed the structure of polymer **BTFMA-DPE**, with the similarity of its spectra to those of
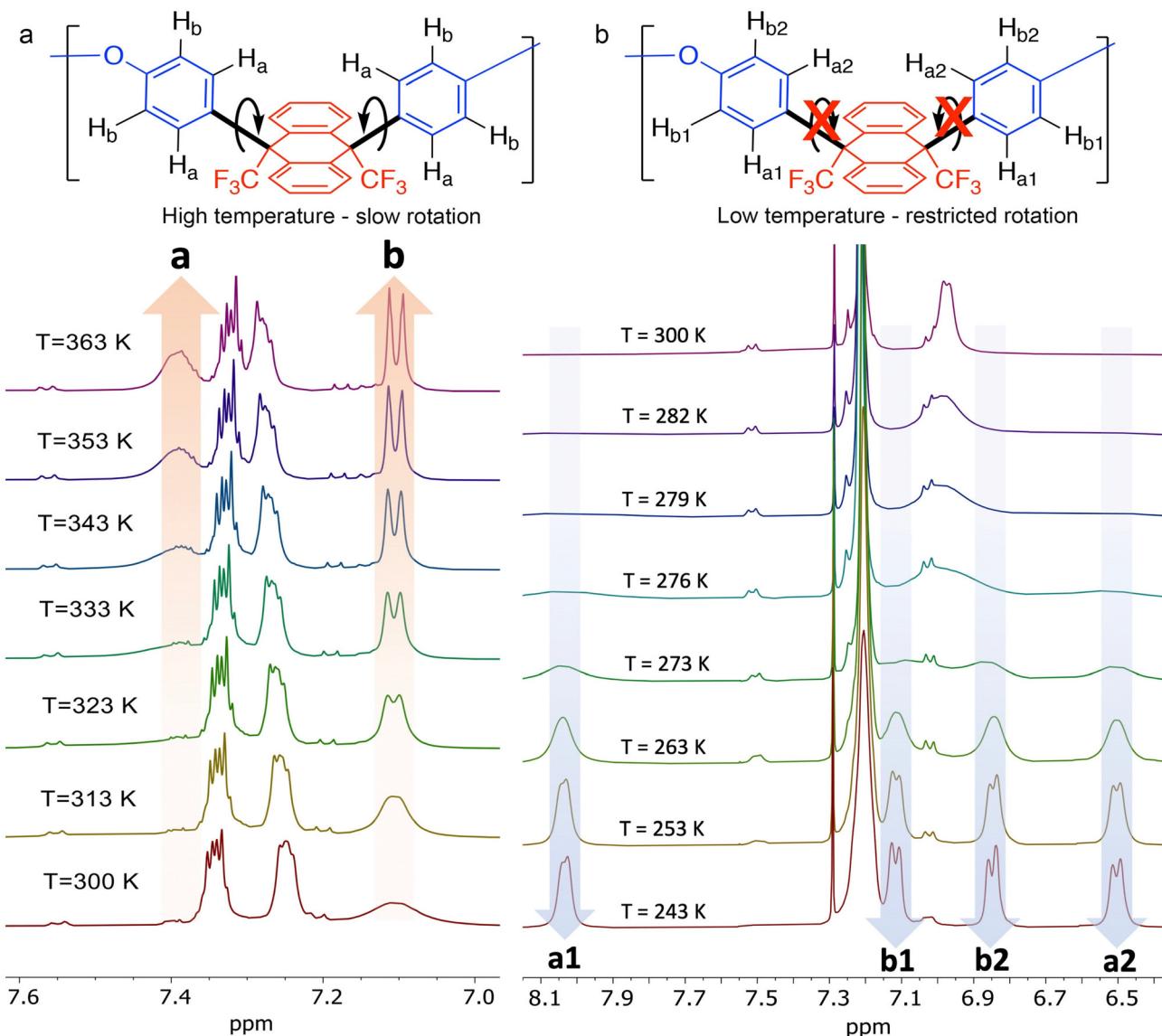
Fig. 3 Variable temperature NMR of polymer **BTFMA-DPE** acquired in the ranges (a) 300−363 K (in DMF-d$_7$) and (b) 243−300 K (in CDCl$_3$). Due to hindered rotation of the benzene rings of the DE monomeric unit, the peak for the hydrogens (H$_a$) adjacent to the new bond only becomes distinct at higher temperatures. At lower temperatures, rotation is frozen so that each of the protons H$_{a1}$, H$_{a2}$, H$_{b1}$ and H$_{b2}$ show a distinct peak.

model compound **1** indicating that there was selective substitution of **DPE** at the *para*-sites relative to its oxygen linker. This also confirms that there is a predominantly "*cis*" arrangement of the CF$_3$ substituents relative to the dihydroanthracene plane, however, it is possible that the two weak doublet peaks observed at ~7.55 and 7.20 ppm in DMF-d$_7$ (Fig. 3a) and at 7.50 and 7.05 ppm in CDCl$_3$ (Fig. 3b) may arise from a small degree of "*trans*" substitution of the dihydroanthracene unit (<5%).

Variable-temperature ^{1}H-NMR spectroscopy (Fig. 3), provides clear evidence of the restricted rotation of the phenyl groups of the **DPE** monomeric unit within **BTFMA-DPE**. At room temperature, the signals associated with the ^{1}H atoms of the **DPE** monomeric unit adjacent to the newly formed bond

(Fig. 3, H$_a$) are not discernible and those adjacent to the oxygen linker (H$_b$) are severely broadened. At elevated temperatures (>340 K, DMF-d$_7$, Fig. 3a), the former appears as a broad signal centred at ~7.4 ppm and the latter as a well-resolved doublet at 7.12 ppm. In contrast, at lower temperatures (<250 K, CDCl$_3$, Fig. 3b), four well-defined doublets are observed consistent with the frozen rotation of the phenyl groups resulting in a discrete signal for each proton. For example, the ^{1}H atoms of the **DPE** monomeric unit adjacent to the newly formed bond are found at 8.05 and 6.50 ppm (Fig. 3b, H$_{a1}$ and H$_{a2}$), with the large difference in chemical shift caused by their exposure to the deshielding and shielding effects, respectively, of the ring current of the benzene rings within the dihydroanthracene unit. The coalescence tempera-

ture (T_c) of the signals for H_{b1} and H_{b2} (Fig. 3b) is at 275 ± 2 K, corresponding to an activation energy of 54 ± 1 kJ mol^{-1}.[56] This value of T_c for **BTFMA-DPE** is slightly higher than that for model compound **1** (270 ± 2 K), which may be due to the added restrictions to the motion of the phenyl rings because of their incorporation into a polymer chain.

Thermal gravimetric analysis (TGA) of **BTFMA-DPE** indicates no decomposition below 400 °C (ESI Fig. 6a†), with initial mass loss occurring at ~430 °C, and no thermal transitions are discernible using differential scanning calorimetry (DSC) below this temperature (ESI Fig. 6b†). The rigidity of the components of this predominantly aromatic polymer will likely ensure a very high glass transition temperature (T_g), which will require further analysis using rapid scanning DSC techniques to determine its value.[57,58] Colourless solutions of **BTFMA-DPE** in chloroform were used to cast robust, flexible, optically clear, self-standing films (Fig. 4) that could be used for gas permeability studies.

Gas adsorption and permeability are routinely used to assess the presence of free volume in a glassy polymer. The powdered form of **BTFMA-DPE** showed significant N_2 and CO_2 adsorption (ESI Fig. 7†) with N_2 uptake at 77 K allowing an apparent SA_{BET} of 450 m^2 g^{-1} and total pore volume of 0.31 ml g^{-1} to be estimated. Although these values are modest compared to those of polymers of intrinsic microporosity (PIMs, *e.g.*, the archetypal **PIM-1** has an apparent SA_{BET} of ~850 m^2 g^{-1} and total pore volume of 0.40 ml g^{-1}),[59] they indicate that **BTFMA-DPE** contains a significant amount of free volume.

The potential of a new polymer for making a membrane to separate a particular gas pair (x/y) is assessed by its per-

Fig. 4 A robust, optically clear, self-standing film of **BTFMA-DPE** fabricated from chloroform solution using the techniques of simple solvent-casting (5 cm diameter, 100 μm thick).

meability (P_x) and ideal selectivity (P_x/P_y). The values for He, H_2, O_2, CO_2, CH_4 and N_2 permeabilities were measured for a self-standing film of **BTFMA-DPE** and can be compared with those from two related polymers, **TFA-DPE** and **TFAP-DPE**,[11,12] prepared using **DPE** by a superacid catalysed polymerisation with 1,1,1-trifluoroacetone and 1,1,1-trifluoroacetophenone, respectively (Table 1). The permeability of **BTFMA-DPE** is much higher for all gases by a factor of 30–80. In addition, the ideal selectivities of **BTFMA-DPE** for the separation of the important gas pairs O_2/N_2 and CO_2/CH_4 are similar to those of **TFAP-DPE**, **TFA-DPE**, and **PIM-1** but at a lower permeability for the latter, which is consistent with the lower values of N_2 and CO_2 adsorption noted above. Generally, polymers suffer from the well-established trade-off between gas permeability and selectivity and the performance of a new polymer is best assessed by considering the position of its data on Robeson plots relative to upper bounds, which were defined using data from the best performing PIMs.[60,62] As shown for the Robeson plots of O_2/N_2 and CO_2/CH_4 (Fig. 5a and b, respectively), the gas permeability data for **BTFMA-DPE** lie close to the 1991 upper bounds for several gas pairs (also H_2/N_2 and H_2/CH_4),[63] unlike those of **TFA-DPE** and **TFAP-DPE**. Whilst modest when compared to that of some PIMs, the permeability of **BTFMA-DPE** is similar to that of the best performing polyimides such as **6FDA-durene**[64] but with greater selectivity for key gas pairs (Table 1). Therefore, the performance of **BTFMA-DPE** is encouraging for a readily processed polymer that can be made easily on a large scale from readily available monomers as is the case for polymer **6FDA-durene**. In addition, it is likely that replacing **DPE** as co-monomer, which possesses unrestricted rotational freedom about the ether linkage, with a conformationally locked monomer will result in a **BTFMA** based polymer with greater intrinsic microporosity. Such work and other initiatives to fulfil the potential of this new monomer for making membrane materials are ongoing.

To conclude, **BTFMA** is a readily prepared monomer that has been demonstrated to undergo efficient polymerisation mediated by a superacid. When copolymerised with **DPE**, a rigid polymer with good film-forming properties is rapidly produced. It is anticipated that **BTFMA** has excellent potential for enhancing the permeability of membrane-forming polymers that are produced using superacid polymerisations by the introduction of greater free volume.

Table 1 Gas permeabilities (P_x, barrer; 1 barrer = 10^{-10} cm$^3_{STP}$ cm cm^{-2} s^{-1} cm Hg^{-1}) and ideal selectivities (P_x/P_y) of **BTFMA-DPE** and related polymers **TFA-DPE** and **TFAP-DPE** measured at 25 °C and 1 bar of feed pressure. For comparison, the values for **PIM-1**[61] and polyimide **6FDA-durene**[64] are included with the former being used to help define the 2008 Robeson upper bounds[60] (Fig. 5)

Polymer	Permeability P_x (barrer)						Ideal selectivity P_x/P_y					
	N_2	O_2	CO_2	CH_4	H_2	He	CO_2/CH_4	CO_2/N_2	O_2/N_2	H_2/N_2	H_2/CH_4	He/N_2
BTFMA-DPE	22.9	97.6	473	22.3	463	327	21.7	21.7	4.26	20.2	20.7	14.3
TFA-DPE[11]	0.7	3.5	17.0	0.7	28.0	29.0	26.2	24.6	5.01	40.1	43.1	42.0
TFAP-DPE[12]	0.4	2.1	8.7	0.4	20	27	22.0	19.5	4.70	44.7	50.6	60.4
PIM-1[61]	92	380	2300	125	1300	660	25.0	21.1	4.0	14.1	10.6	7.2
6FDA-durene[64]	39	135	678	38	585	355	20.2	17.4	3.46	15.0	15.4	9.1
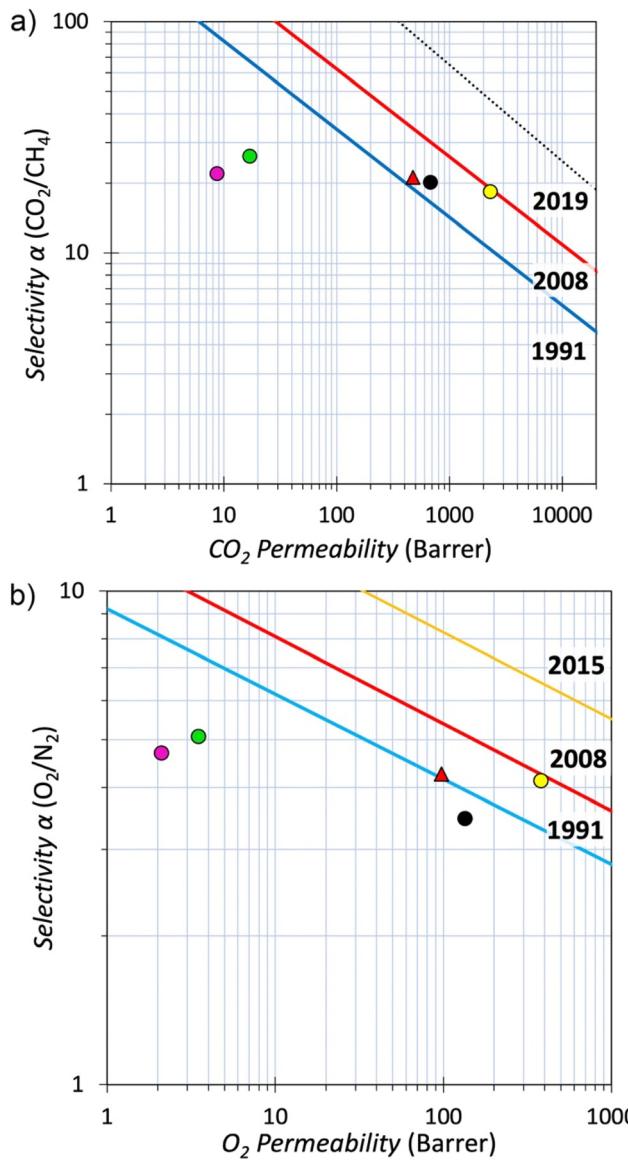
Fig. 5 Robeson plots for a) CO_2/CH_4 and b) O_2/N_2 showing the data for **BTFMA-DPE** (red) and structurally related polymers **TFA-DPE** (green) and **TFAP-DPE** (purple). For comparison, the data points are also provided for **PIM-1** [60,61] (yellow) and the much-studied polyimide **6FDA-durene (black)**.[64]

Acknowledgements

Data availability

The data supporting this article have been included as part of the ESI.† Crystallographic data for model compound **1** has been deposited at the CCDC with the accession number 2382285† and can be obtained from **https://www.ccdc.cam.ac.uk/structures/**.

Conflicts of interest

There are no conflicts to declare.

References

1 H. M. Colquhoun, M. G. Zolotukhin, L. M. Khalilov and U. M. Dzhemilev, *Macromolecules*, 2001, **34**, 1122–1124.

2 M. Zolotukhin, S. Fomine, R. Salcedo and L. Khalilov, *Chem. Commun.*, 2004, 1030–1031.

3 M. G. Zolotukhin, L. Fomina, R. Salcedo, L. E. Sansores, H. M. Colquhoun and L. M. Khalilov, *Macromolecules*, 2004, **37**, 5140–5141.

4 L. I. Olvera, M. T. Guzmán-Gutiérrez, M. G. Zolotukhin, S. Fomine, J. Cárdenas, F. A. Ruiz-Trevino, D. Villers, T. A. Ezquerra and E. Prokhorov, *Macromolecules*, 2013, **46**, 7245–7256.

5 A. M. Diaz, M. G. Zolotukhin, S. Fomine, R. Salcedo, O. Manero, G. Cedillo, V. M. Velasco, M. T. Guzman, D. Fritsch and A. F. Khalizov, *Macromol. Rapid Commun.*, 2007, **28**, 183–187.

6 M. G. Zolotukhin1, S. Fomine, L. M. Lazo, M. D. C. G. Hernández, M. T. Guzmán-Gutiérrez, A. Ruiz-Trevino, D. Fritsch, D. C. Cuellas and J. M. Fernandez-G, *High Perform. Polym.*, 2007, **19**, 638–648.

7 A. R. Cruz, M. G. Zolotukhin, S. L. Morales, J. Cardenas, G. Cedillo, S. Fomine, M. Salmon and M. P. Carreón-Castro, *Chem. Commun.*, 2009, 4408–4410.

8 E. Cetina-Mancilla, L. I. Olvera, J. Balmaseda, M. Forster, F. A. Ruiz-Treviño, J. Cárdenas, E. Vivaldo-Lima and M. G. Zolotukhin, *Polym. Chem.*, 2020, **11**, 6194–6205.

9 Y. Jin, T. Wang, X. Che, J. Dong, Q. Li and J. Yang, *J. Power Sources*, 2022, **526**, 231131.

10 M. G. Zolotukhin, S. Fomine, L. M. Lazo, R. Salcedo, L. E. Sansores, G. G. Cedillo, H. M. Colquhoun, J. M. Fernandez-G and A. F. Khalizov, *Macromolecules*, 2005, **38**, 6005–6014.

11 M. T. Guzmán-Gutiérrez, M. G. Zolotukhin, D. Fritsch, F. A. Ruiz-Treviño, G. Cedillo, E. Fregoso-Israel, C. Ortiz-Estrada, J. Chavez and C. Kudla, *J. Membr. Sci.*, 2008, **323**, 379–385.

12 M. T. Guzmán-Gutiérrez, M. H. Rios-Dominguez, F. A. Ruiz-Treviño, M. G. Zolotukhin, J. Balmaseda, D. Fritsch and E. Prokhorov, *J. Membr. Sci.*, 2011, **385–386**, 277–284.

13 E. C. Mancilla, H. Hernández-Martínez, M. G. Zolotukhin, F. A. Ruiz-Treviño, M. O. González-Díaz, J. Cardenas and U. Scherf, *Ind. Eng. Chem. Res.*, 2019, **58**, 15280–15287.

14 H. Hernández-Martínez, E. Coutino-Gonzalez, F. Espejel-Ayala, F. A. Ruiz-Treviño, G. Guerrero-Heredia, A. L. García-Riego and L. I. Olvera, *ACS Omega*, 2021, **6**, 4921–4931.

15 I. Hossain, A. Husna, I. Jeong and T.-H. Kim, *ACS Appl. Polym. Mater.*, 2022, **4**, 3779–3790.

16 L. Matesanz-Niño, N. Esteban, M. T. Webb, A. Martínez-Gómez, F. Suárez-García, A. González-Ortega, J. A. Miguel, L. Palacio, M. Galizia, C. Álvarez and Á. E. Lozano, *Polymer*, 2023, **267**, 125647.

17 Y. Dou, X. Dong, Y. Ma, P. Ge, C. Li, A. Zhu, Q. Liu and Q. Zhang, *J. Membr. Sci.*, 2022, **659**, 120779.

18 S. Fang, H. Tang, M. Wang, Z. Xu and N. Li, *J. Membr. Sci.*, 2023, **676**, 121620.

19 X. Du, Z. Wang, H. Zhang, Y. Yuan, H. Wang and Z. Zhang, *J. Membr. Sci.*, 2021, **619**, 118805.

20 L. Xu, H. Wang, L. Min, W. Xu and W. Zhang, *Sep. Purif. Technol.*, 2023, **312**, 123396.

21 W.-H. Lee, Y. S. Kim and C. Bae, *ACS Macro Lett.*, 2015, **4**, 814–818.

22 E. J. Park, P. Jannasch, K. Miyatake, C. Bae, K. Noonan, C. Fujimoto, S. Holdcroft, J. R. Varcoe, D. Henkensmeier, M. D. Guiver and Y. S. Kim, *Chem. Soc. Rev.*, 2024, **53**, 5704–5780.

23 J. S. Olsson, T. H. Pham and P. Jannasch, *Adv. Funct. Mater.*, 2018, **28**, 1702758.

24 J. Wang, Y. Zhao, B. P. Setzler, S. Rojas-Carbonell, C. Ben Yehuda, A. Amel, M. Page, L. Wang, K. Hu, L. Shi, S. Gottesfeld, B. Xu and Y. Yan, *Nat. Energy*, 2019, **4**, 392–398.

25 D. Pan, T. H. Pham and P. Jannasch, *ACS Appl. Energy Mater.*, 2021, **4**, 11652–11665.

26 T. Ryu, H. Jang, F. Ahmed, N. S. Lopa, H. Yang, S. Yoon, I. Choi and W. Kim, *Int. J. Hydrogen Energy*, 2018, **43**, 5398–5404.

27 W. Li, R. Zhang, X. Zhao, Z. Yue, H. Qian and H. Yang, *J. Mater. Chem. A*, 2023, **11**, 4547–4558.

28 Y. Jin, T. Wang, X. Che, J. Dong, R. Liu and J. Yang, *J. Membr. Sci.*, 2022, **641**, 119884.

29 W. Yu, Z. Ge, K. Zhang, X. Liang, X. Ge, H. Wang, M. Li, X. Shen, Y. Xu, L. Wu and T. Xu, *Ind. Eng. Chem. Res.*, 2022, **61**, 4329–4338.

30 J. Li, C. Yang, X. Zhang, Z. Xia, S. Wang, S. Yu and G. Sun, *J. Mater. Chem. A*, 2023, **11**, 18409–18418.

31 H. Bai, H. Peng, Y. Xiang, J. Zhang, H. Wang, S. Lu and L. Zhuang, *J. Power Sources*, 2019, **443**, 227219.

32 S. Zhang, X. Zhu and C. Jin, *J. Mater. Chem. A*, 2019, **7**, 6883–6893.

33 N. Chen, C. Hu, H. H. Wang, S. P. Kim, H. M. Kim, W. H. Lee, J. Y. Bae, J. H. Park and Y. M. Lee, *Angew. Chem., Int. Ed.*, 2021, **60**, 7710–7718.

34 N. Chen, S. Y. Paek, J. Y. Lee, J. H. Park, S. Y. Lee and Y. M. Lee, *Energy Environ. Sci.*, 2021, **14**, 6338–6348.

35 Y. Zhao, Y. Yang, S. Wang, T. Wang, C. Liu, S. Cheng, H. Wei and Y. Ding, *J. Membr. Sci.*, 2023, **688**, 122132.

36 L. W. Lai, H. Peng, Y. N. Ding, X. B. Yue, Q. G. Zhang, A. M. Zhu and Q. L. Liu, *J. Membr. Sci.*, 2024, **703**, 122837.

37 J. Xue, J. C. Douglin, K. Yassin, T. Huang, H. Jiang, J. Zhang, Y. Yin, D. R. Dekel and M. D. Guiver, *Joule*, 2024, **8**, 1457–1477.

38 X. Yan, H. Zhang, Z. Hu, L. Li, L. Hu, Z. A. Li, L. Gao, Y. Dai, X. Jian and G. He, *ACS Appl. Mater. Interfaces*, 2019, **11**, 44315–44324.

39 W. Tang, T. Mu, X. Che, J. Dong and J. Yang, *ACS Sustainable Chem. Eng.*, 2021, **9**, 14297–14306.

40 Y. Wang, H. Peng, M. Hu, L. Zhuang, J. Lu and L. Xiao, *J. Power Sources*, 2021, **486**, 229376.

41 Z. Xu, Y. Liao, M. Pang, L. Wan, Q. Xu, Y. Zhen and B. Wang, *Energy Environ. Sci.*, 2023, **16**, 3815–3824.

42 E. J. Park, C. B. Capuano, K. E. Ayers and C. Bae, *J. Power Sources*, 2018, **375**, 367–372.

43 X. Cheng, C. Li, X. Zou, B. Sun, L. Wang, W. Wang and X. Meng, *Chem. Eng. J.*, 2024, **483**, 149328.

44 X. Su, S. Nan, Y. Gu, W. Wei and R. He, *Chem. Eng. J.*, 2024, **482**, 149056.

45 G. K. S. Prakash and A. K. Yudin, *Chem. Rev.*, 1997, **97**, 757–786.

46 B. C. Ahvazi and D. S. Argyropoulos, *J. Agric. Food Chem.*, 1996, **44**, 2167–2175.

47 R. P. Singh and J. N. M. Shreeve, *J. Fluorine Chem.*, 2012, **133**, 20–26.

48 S. Yamada, K. Kinoshita, S. Iwama, T. Yamazaki, T. Kubota and T. Yajima, *RSC Adv.*, 2013, **3**, 6803–6806.

49 F. Li, J. Liu, X. Liu, Y. Wang, X. Gao, X. Meng and G. Tu, *Polymers*, 2018, **10**, 546.

50 Y. Wang, Y. Li, F. Li, J. Shen, J. Zhao and G. Tu, *Polym. Test.*, 2023, **129**, 108269.

51 O. V. Khoroshilova, I. A. Boyarskaya and A. V. Vasilyev, *J. Org. Chem.*, 2022, **87**, 15845–15862.

52 O. V. Khoroshilova and A. V. Vasilyev, *J. Org. Chem.*, 2020, **85**, 5872–5883.

53 M. J. O'Connor, K. N. Boblak, M. J. Topinka, P. J. Kindelin, J. M. Briski, C. Zheng and D. A. Klumpp, *J. Am. Chem. Soc.*, 2010, **132**, 3266–3267.

54 A. Cruz-Rosado, J. E. Romero-Hernández, M. Ríos-López, S. López-Morales, G. Cedillo, L. M. Ríos-Ruiz, E. Cetina-Mancilla, J. Palacios-Alquisira, M. G. Zolotukhin and E. Vivaldo-Lima, *Polymer*, 2022, **243**, 124616.

55 M. T. Guzmán-Gutiérrez, D. R. Nieto, S. Fomine, S. L. Morales, M. G. Zolotukhin, M. C. G. Hernandez, H. Kricheldorf and E. S. Wilks, *Macromolecules*, 2011, **44**, 194–202.

56 M. T. Huggins, T. Kesharwani, J. Buttrick and C. Nicholson, *J. Chem. Educ.*, 2020, **97**, 1425–1429.

57 H. J. Yin, Y. Z. Chua, B. Yang, C. Schick, W. J. Harrison, P. M. Budd, M. Bohning and A. Schonhals, *J. Phys. Chem. Lett.*, 2018, **9**, 2003–2008.

58 H. Yin, B. Yang, Y. Z. Chua, P. Szymoniak, M. Carta, R. Malpass-Evans, N. B. McKeown, W. J. Harrison, P. M. Budd, C. Schick, M. Böhning and A. Schönhals, *ACS Macro Lett.*, 2019, **8**, 1022–1028.

59 P. M. Budd, B. S. Ghanem, S. Makhseed, N. B. McKeown, K. J. Msayib and C. E. Tattershall, *Chem. Commun.*, 2004, 230–231.

60 L. M. Robeson, *J. Membr. Sci.*, 2008, **320**, 390–400.

61 P. M. Budd, K. J. Msayib, C. E. Tattershall, B. S. Ghanem, K. J. Reynolds, N. B. McKeown and D. Fritsch, *J. Membr. Sci.*, 2005, **251**, 263–269.

62 B. Comesaña-Gándara, J. Chen, C. G. Bezzu, M. Carta, I. Rose, M.-C. Ferrari, E. Esposito, A. Fuoco, J. C. Jansen and N. B. McKeown, *Energy Environ. Sci.*, 2019, **12**, 2733–2740.

63 L. M. Robeson, *J. Membr. Sci.*, 1991, **62**, 165–185.

64 W.-H. Lin and T.-S. Chung, *J. Membr. Sci.*, 2001, **186**, 183–193.